

RESEARCH ARTICLE

Influence of N6-methyladenosine (m6A) modification on cell phenotype in Alzheimer's disease

Pengyun Ni^{1*}, Kaiting Pan², Bingbing Zhao³

1 Department of Science and Education, Baoji Traditional Chinese Medicine Hospital, Baoji, Shannxi, P.R China, **2** Department of Neurology, Baoji Third Hospital, Baoji, Shannxi, P.R China, **3** Emergency Department, Baoji Traditional Chinese Medicine Hospital, Baoji, Shannxi, P.R China

✉ These authors contributed equally to this work.

* 469079448@qq.com



Abstract

Objective

Recent research has suggested that m6A modification takes on critical significance to Neurodegeneration. As indicated by the genome-wide map of m6A mRNA, genes in Alzheimer's disease model achieved significant m6A methylation. This study aimed to investigate the hub gene and pathway of m6A modification in the pathogenesis of AD. Moreover, possible brain regions with higher gene expression levels and compounds exerting potential therapeutic effects were identified. Thus, this study can provide a novel idea to explore the treatment of AD.

Methods

Differential expression genes (DEGs) of GSE5281 and GSE48350 from the Gene Expression Omnibus (GEO) database were screened using the Limma package. Next, the enrichment analysis was conducted on the screened DEGs. Moreover, the functional annotation was given for N6-methyladenosine (m6A) modification gene. The protein-protein interaction network (PPI) analysis and the visualization analysis were conducted using STRING and Cytoscape. The hub gene was identified using CytoHubba. The expression levels of Hub genes in different regions of brain tissue were analyzed based on Human Protein Atlas (HPA) database and Bgee database. Subsequently, the candidate drugs targeting hub genes were screened using cMAP.

Results

A total of 42 m6A modified genes were identified in AD (20 up-regulated and 22 down-regulated genes). The above-described genes played a certain role in biological processes (e.g., retinoic acid, DNA damage response and cysteine-type endopeptidase activity), cellular components (e.g., mitochondrial protein complex), and molecular functions (e.g., RNA methyltransferase activity and ubiquitin protein ligase). KEGG results suggested that the above-mentioned genes were primarily involved in the Hippo signaling pathway of

OPEN ACCESS

Citation: Ni P, Pan K, Zhao B (2023) Influence of N6-methyladenosine (m6A) modification on cell phenotype in Alzheimer's disease. PLoS ONE 18(8): e0289068. <https://doi.org/10.1371/journal.pone.0289068>

Editor: Divakar Sharma, Lady Hardinge Medical College, INDIA

Received: November 21, 2022

Accepted: July 11, 2023

Published: August 7, 2023

Peer Review History: PLOS recognizes the benefits of transparency in the peer review process; therefore, we enable the publication of all of the content of peer review and author responses alongside final, published articles. The editorial history of this article is available here: <https://doi.org/10.1371/journal.pone.0289068>

Copyright: © 2023 Ni et al. This is an open access article distributed under the terms of the [Creative Commons Attribution License](#), which permits unrestricted use, distribution, and reproduction in any medium, provided the original author and source are credited.

Data Availability Statement: All Expressions of GSE5281 and GSE48350, gene of m6A datas are available from the Figshare database. (DOI: [10.6084/m9.figshare.22656136](https://doi.org/10.6084/m9.figshare.22656136), URL: <https://figshare.com/account/home>).

Funding: The authors received no specific funding for this work.

Competing interests: The authors have declared that no competing interests exist.

neurodegeneration disease. A total of 10 hub genes were screened using the protein-protein interaction network, and the expression of hub genes in different regions of human brain was studied. Furthermore, 10 compounds with potential therapeutic effects on AD were predicted.

Conclusion

This study revealed the potential role of the m6A modification gene in Alzheimer's disease through the bioinformatics analysis. The biological changes may be correlated with retinoic acid, DNA damage response and cysteine-type endopeptidase activity, which may occur through Hippo signaling pathway. The hub genes (SOX2, KLF4, ITGB4, CD44, MSX1, YAP1, AQP1, EGR2, YWHAZ and TFAP2C) and potential drugs may provide novel research directions for future prognosis and precise treatment.

Introduction

Alzheimer's disease (AD) has been confirmed as one of the most common Neurodegeneration, characterized by a progressive decline in memory function and even cognitive impairment [1]. AD has a high incidence in the elderly population and in some countries [2]. Besides, AD is recognized as a problem that should arouse the attention of the society and the government. Due to the lack of effective treatment, AD patients and their families are currently subjected to considerable number of inconvenience and health risks. The pathogenesis and therapy of AD should be urgently studied.

N6-methyladenosine (m6A) refers to a common reversible methylation modification, including methylation, demethylation, and recognition of RNA Post-transcriptional modification [3]. Existing research has confirmed that m6A extensively exists in mammals, with an average of 3–5 M6A sites per mRNA transcript on isolated RNA adenosine [4]. m6A is capable of disrupting chromatin-modifying enzyme-associated transcript stability and thereby regulate histone modifications [5]. m6A influences mRNA metabolism by regulating RNA degradation [6], translation [7], RNA splicing [8] and nuclear export [9] through multiple types of protein complexes. In animals, known methyltransferase protein complexes include methyltransferase protein 3 (METTL3) and METTL14, which interact with METTL14 to form heterodimers that exert methyltransferase activity [10–12]. m6A removal is mainly accomplished by removal of the protein AlkB homologue 5(Alkbh5) and the obesity-associated protein FTO [10, 13]. The decoding of m6A labeling is performed by YTHDF1/2/3, YTHDC1/2, hnRNP a 2/B 1 and RNA binding proteins [6, 10, 13–17].

m6A refers to a reversible RNA modification [18] occurring in the brain [19], and it plays a certain role in the physiological functions of neurogenesis [5], learning and memory [20]. Existing research has suggested that mutations in a wide variety of m6A participants are correlated with neurological disorders [21]. The methylation level of m6A was significantly increased in the AD model, suggesting that m6A may play a key role in AD [22]. However, the mechanism of m6A in the brain is still not perfect and needs further study.

In this study, the data were collected from public databases, and bioinformatics methods were adopted to explore m6A-modified hub genes and pathways in Alzheimer's disease. This study aimed to further clarify the expression of key genes in a wide variety of brain regions and predict potential therapeutic compounds, so as to explore novel ideas and lay a research basis for the treatment of AD.

Materials and methods

Data acquisition and processing

Two microarray datasets (GSE5281 and GSE48350) were downloaded in this study from the Gene Expression Omnibus (GEO) database [23] (<http://www.ncbi.nlm.nih.gov/gds/>) investigating gene expression profiles changes in patients with Alzheimer's disease.

The gene expression profile GSE5281 and GSE48350 were generated on the platform of GPL570 [HG-U133_Plus_2] Affymetrix Human Genome U133 Plus 2.0 Array. This dataset comprises 247 control samples and 167 AD samples.

Analysis of differentially expressed genes (DEGs)

GSE5281 and GSE48350 were downloaded from the GEO database using the GEO query package [24] to remove one probe for multiple molecules. When a probe corresponding to the same molecule is encountered, only the probe with the largest signal value will be retained. Subsequently, Limma package [25] was adopted to analyze the difference between the two groups. Volcano plots were drawn using fold change and corrected p-values. $|\log_2(\text{Fold Change})| > 0.58$ and $\text{P.value} < 0.05$ were considered the threshold for the DEGs. The expression heatmaps were exhibited using the R package pheatmap [26].

N6-methyladenosine (m6A) modification gene and Venn analysis

The GeneCards database [27] (<https://www.Genecards.org/>) was searched for relevant genes with the keywords "m6A" and "N6-methyladenosine", and the organisms were set as "homo sapiens". Subsequently, the Venn diagram between AD up-regulated and down-regulated DEGs and m6A genes was generated using Bioinformatics (<http://www.bioinformatics.com.cn/>). Next, the overlapping genes of DEGs and m6A were analyzed.

Next, the expression differences of the overlapping genes between the AD group and the control group were visualized using PCA maps. On that basis, the individuals of up-regulated gene and down-regulated gene expression was proved.

Gene ontology (GO) enrichment analysis and Kyoto encyclopedia of genes and genomes (KEGG) pathway analysis

Metascape [28] (<https://Metascape.org/gp/index.html#/main/step1>) and Bioinformatics were adopted to study the enrichment of overlapping genes by process and pathway. The GO terms for Biological Process (BP), Cellular Component (CC), and Molecular Function (MF) categories were enriched using the Metascape online tool. The biological processes, cellular components, molecular functions and KEGG pathway enrichment analysis of the overlapping genes were identified with the human genome as a background reference and $\text{P value} < 0.05$ as the inclusion criteria.

PPI network construction and module analysis

The STRING database (<https://cn.string-db.org/>) refers to a tool for assessing functional protein-protein interactions (PPI) [29]. A PPI network of overlapping genes was built on STRING 11.5 to predict interactions between proteins encoded by genes that take on critical significance to m6A modification in AD. Subsequently, the PPI data was imported into Cytoscape 3.7.2 software [30] for visualization, and the Hub gene was screened out using the CytoHubba [31] plug-in.

Selection and analysis of hub genes

The top 10 core genes were screened using CytoHubba, a plugin in Cytoscape software. The Protein expression profiles of hub genes on the tissue level and the gene expression level originated from the HPA (Human Protein Atlas) database. The gene expression scores of hub genes on the tissue level originated from the Bgee database (<https://bgee.org>).

Identification and verification of hub genes

We brought hub genes into the GSE5281 and GSE48350 datasets to identify and validate hub genes expression levels and diagnostic value. We visualized the gene expression levels of the hub genes between AD patients and healthy controls using a Box graph and Scatter plot. AUCs were calculated by receiver operating characteristic (ROC) curve analysis to determine the predictive value of hub genes.

Screening for potential pharmacological targets

In this study, compounds with potential therapeutic effects on AD were predicted using the CMAP database [32] (ConnectivityMap, <https://clue.io/query>). The CMAP database can be adopted for the comparison of similarity between drug-induced gene profiles and gene expression. Scores over 0 represent the small-molecule compounds similar to those for monitoring gene changes, while scores less than 0 represent the small-molecule compounds with opposite effects on genes to be tested that may exert therapeutic effects on disease. Screening for compounds with connectivity score less than -80 is recognized as a reliable prediction. Through the comparison of the Gene expression profiling data between the compounds and cell lines, compounds with fractions less than 0 were identified as having potential therapeutic effects on AD. Thus, as indicated by the comparison of the Gene expression profiling data between the compounds and cell lines, compounds with a score of less than -80 that may have potential therapeutic effects on AD should be screened.

Result

Identification of DEGs during AD

The differential gene expression analysis between samples was performed to compare the difference in gene expression between the AD group and the control group. The gene dataset GSE5281 and GSE48350 contained a total of 167 Alzheimer's disease samples and 247 normal samples. With the Limma package for differential expression analysis, with $|\log_2(\text{Fold Change})| > 0.58$ and $P.\text{value} < 0.05$ as the screening conditions, 917 differently expressed genes in brain tissues of AD patients were identified, as compared with normal brain tissues. To be specific, 265 were up-regulated, and 652 were down-regulated, and the clustering analysis of the above-described differential genes was conducted, with the result illustrated in the volcano plot (Fig 1A). Fig 1B presents a heat map of data set, suggesting that the clustering of samples is highly reliable.

M6A modification gene and Venn analysis

In this study, 1126 m6A genes were identified by searching GeneCards and BioGPS databases. AD up-regulated and down-regulated DEGs gene and m6A gene were introduced into the Venn analysis tool. There were 42 overlapping genes, comprising 20 up-regulated overlapping genes and down-regulated 22 overlapping genes (Fig 2A). Furthermore, as depicted in the PCA plot, the control group and AD group samples were separated, suggesting that the

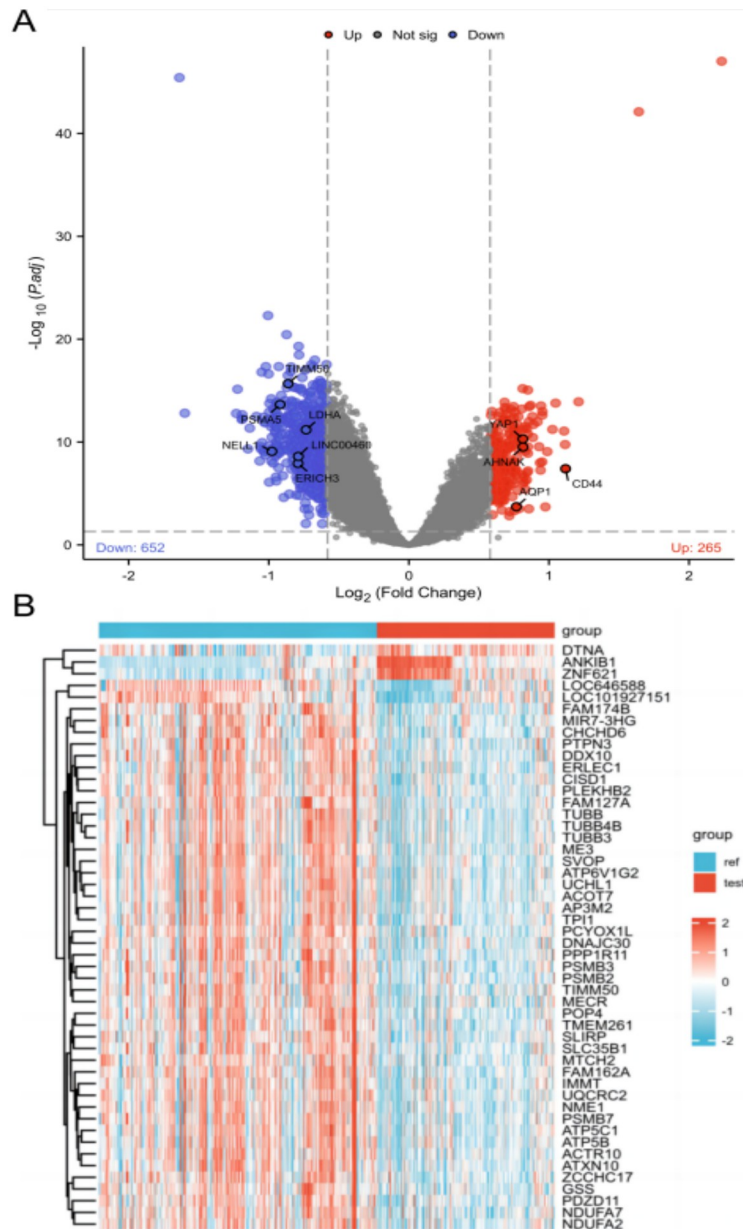


Fig 1. Differential expressed gene (DEG) analysis on Alzheimer's disease. (A) Volcanic plots of gene expression of Alzheimer's disease in GSE5281 and GSE48350. Red represents upregulated DEGs, blue represents downregulated DEGs. $P < 0.5$, $|\log_2(\text{Fold Change})| > 0.58$. (B) Heat map of the DEGs. Showing the 50 differentially expressed genes. Red color represents up-regulated genes, and blue represents down-regulated genes.

<https://doi.org/10.1371/journal.pone.0289068.g001>

expression of up-regulated and down-regulated overlapping genes different between the AD Group and the control group (Fig 2B).

GO and KEGG Pathway enrichment analysis

The GO and KEGG enrichment analysis was conducted on the overlapping genes to study the function of the overlapping genes of AD DEGs and m6A gene. As indicated by the GO

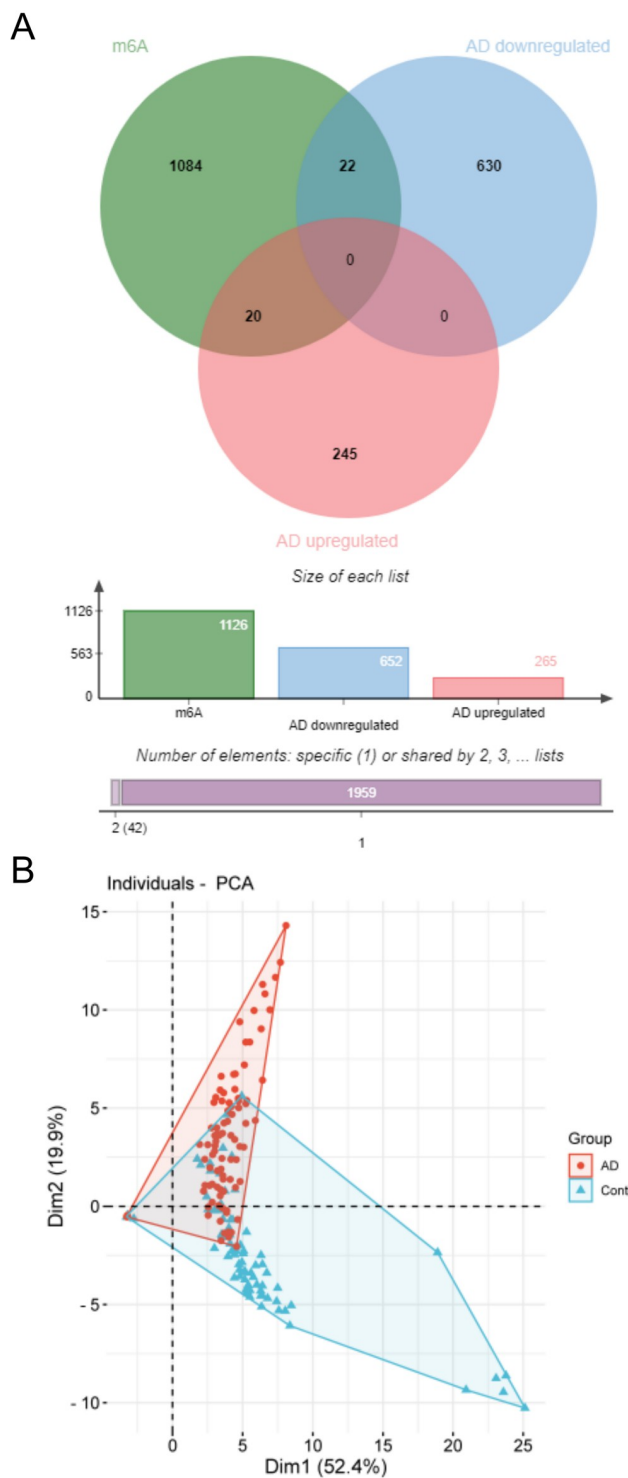


Fig 2. Overlapping genes. (A) Venn diagram of the overlapping genes of AD DEGs and m6A gene. Red represents upregulated DEGs, blue represents downregulated DEGs. (B) PCA indicates that the control group and AD group samples were separated, suggesting that there were differences in gene expression of up-regulated and down-regulated overlapping genes different between the groups.

<https://doi.org/10.1371/journal.pone.0289068.g002>

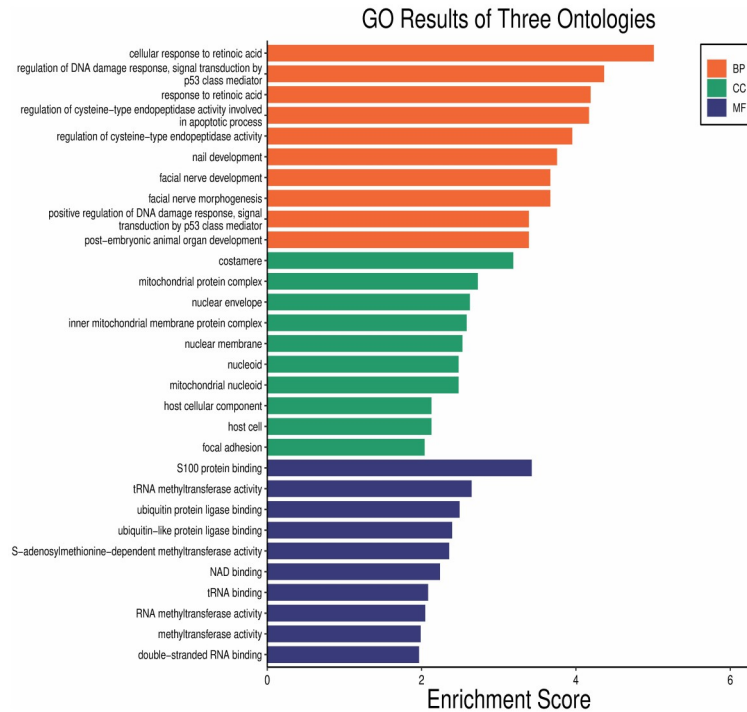


Fig 3. GO analysis of the overlapping genes of AD DGEs and m6A genes. The bars show the Top10 processes enriched by overlapping genes in BP, CC and MF.

<https://doi.org/10.1371/journal.pone.0289068.g003>

analysis results, the overlapping genes were primarily enriched in involving in retinoic acid, DNA damage response, and cysteine-type endopeptidase activity of BP, mitochondrial protein complex of CC, and RNA methyltransferase activity and ubiquitin protein ligase of MF (Fig 3). The top 10 processes with the smallest P-value of three ontologies of BPs, CCs, and MFs enriched by AQP1, MSX1, ITGB4, ADARB1, EEF1E1, KLF4, FXR1, TRMT10C, UQCRC2, NUP93, LRPPRC, AHNK, ATP2A2, YWHAZ, IDH3G, NDUFA13, CCT2, MECOM, PDK4, SOX2, YAP1, CD44, EGR2, LDHA, TIMM50, NELL1, NSUN6, as well as PSMA5 were enriched in three aspects of BPs, CCs and MFs (Fig 4A–4C). The KEGG result indicated the overlapping genes enriched in neurodegeneration disease and Hippo signaling pathway (Fig 5). Table 1 lists the details results of the top five processes of the GO and KEGG enrichment analysis.

PPI network construction and identification of hub genes

The PPI network (the minimum required interaction score set to 0.15) of the overlapping genes (38 nodes, 264 edges) were obtained using Cytoscape (Fig 6A) to investigate the interaction between the proteins corresponding to the overlapping genes. The larger the gene degree value, the larger the point will be. The darker the gene color and the wider the edge, the stronger the evidence for the interaction between proteins will be. The 10 topological methods of the CytoHubba plug-in in Cytoscape were adopted to screen top10 hub genes (i.e., SOX2, KLF4, ITGB4, CD44, MSX1, YAP1, AQP1, EGR2, YWHAZ, and TFAP2C) (Fig 6B, 10 nodes, 36 edges). Table 2 lists the gene symbols, description, and functions.

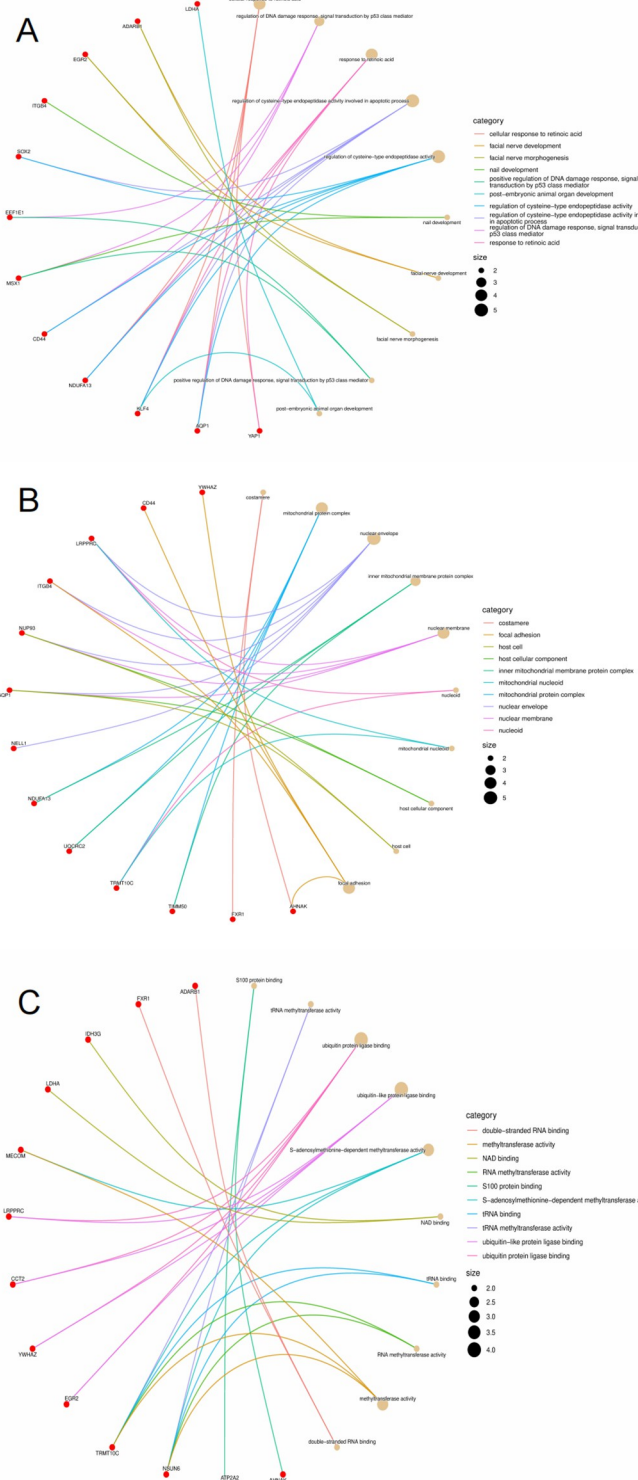


Fig 4. Circle graph in GO enrichment of the overlapping genes of AD DGEs and m6A gene. (A-C) The circle graph shows the overlapping genes enriched in the Top10 GO categories of BP, CC, and MF, respectively. The Go category is represented by a yellow point, the color of the line passed by the point represents the category indicated in the diagram, and the size of the point indicates the number of genes it contains.

<https://doi.org/10.1371/journal.pone.0289068.g004>

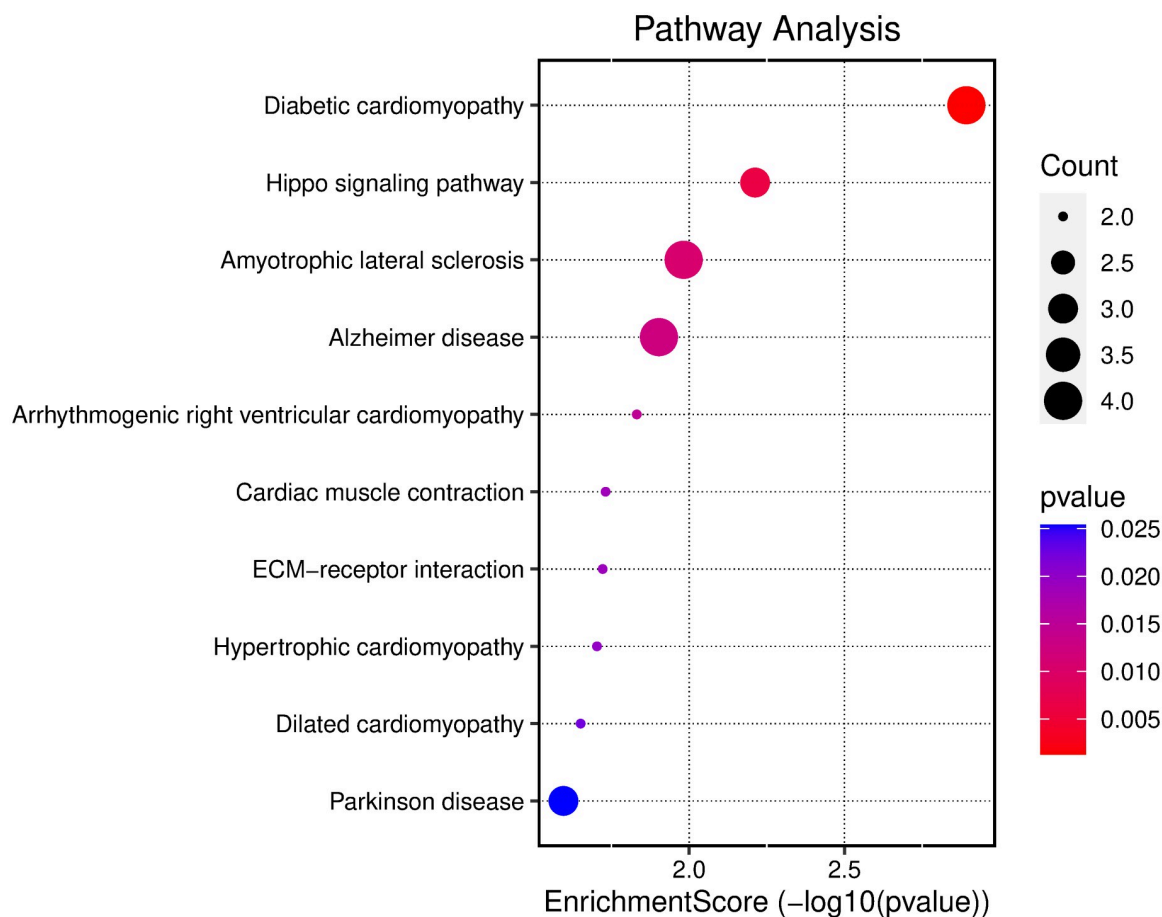


Fig 5. KEGG enrichment analysis of the overlapping genes. KEGG enrichment analysis of the overlapping genes of overlapping genes.
<https://doi.org/10.1371/journal.pone.0289068.g005>

The protein level of hub gene is expressed in different regions of human brain

The samples in GSE5281 and GSE48350 were taken from the human brain tissues. To verify the expression of central genes in different regions of the brain, we compared gene expression levels of hub genes between Cerebral cortex, Hippocampal formation, Thalamus, Hypothalamus, Midbrain, Cerebellum, and White matter in human brain tissues with the HPA database (Fig 7A). As a preliminary reference, the differential expression regions of the above-mentioned genes may exist during the development of AD. The results suggested that hub genes expressed differently in different brain regions. The expression of AQP1 in White matter was the most significant, reaching 432.4 nTPM. However, the expression level ranged from 79.1 nTPM to 181.1 nTPM in other brain regions. The expression levels of YWHAZ in Cerebral cortex and Hippocampal formation reached 343 nTPM and 366.2 nTPM, respectively. The expression levels of CD44 in Hypothalamus, Midbrain and White matter were higher than those in other subregions, ranging from 102.3 nTPM to 116.5 nTPM. The expression levels of SOX2 and KLF4 were between 46.5 nTPM and 104.8 nTPM. The expression levels of MSX1 and YAP1 in different brain regions ranged from 11.8 nTPM to 30.2 nTPM. KLF4 expression, EGR2 and TFAP2C was lower than 10 nTPM.

Table 1. The top 5 processes with results of GO and KEGG enrichment analysis.

	ID	Description	pvalue	geneID	Count
BP	GO:0071300	cellular response to retinoic acid	9.79066E-06	YAP1/AQP1/KLF4/NDUFA13	4
BP	GO:0043516	regulation of DNA damage response, signal transduction by p53 class mediator	4.32091E-05	CD44/MSX1/EEF1E1	3
BP	GO:0032526	response to retinoic acid	6.45273E-05	YAP1/AQP1/KLF4/NDUFA13	4
BP	GO:0043281	regulation of cysteine-type endopeptidase activity involved in apoptotic process	6.77998E-05	CD44/AQP1/KLF4/NDUFA13/SOX2	5
BP	GO:2000116	regulation of cysteine-type endopeptidase activity	0.000111652	CD44/AQP1/KLF4/NDUFA13/SOX2	5
CC	GO:0098798	mitochondrial protein complex	0.001866338	TIMM50/TRMT10C/UQCRC2/NDUFA13	4
CC	GO:0005635	nuclear envelope	0.002366697	NELL1/AQP1/NUP93/ITGB4/LRPPRC	5
CC	GO:0098800	inner mitochondrial membrane protein complex	0.002608254	TIMM50/UQCRC2/NDUFA13	3
CC	GO:0031965	nuclear membrane	0.002959294	AQP1/NUP93/ITGB4/LRPPRC	4
CC	GO:0005925	focal adhesion	0.009143824	CD44/AHNAK/YWHAZ/ITGB4	4
MF	GO:0031625	ubiquitin protein ligase binding	0.00321757	EGR2/YWHAZ/CCT2/LRPPRC	4
MF	GO:0044389	ubiquitin-like protein ligase binding	0.004014383	EGR2/YWHAZ/CCT2/LRPPRC	4
MF	GO:0008757	S-adenosylmethionine-dependent methyltransferase activity	0.004386642	NSUN6/TRMT10C/MECOM	3
MF	GO:0008173	RNA methyltransferase activity	0.008975213	NSUN6/TRMT10C	2
MF	GO:0008168	methyltransferase activity	0.010271748	NSUN6/TRMT10C/MECOM	3
KEGG	hsa05415	Diabetic cardiomyopathy	0.001280589	ATP2A2/UQCRC2/PDK4/NDUFA13	4
KEGG	hsa04390	Hippo signaling pathway	0.006131771	YAP1/YWHAZ/SOX2	3
KEGG	hsa05014	Amyotrophic lateral sclerosis	0.010414549	PSMA5/NUP93/UQCRC2/NDUFA13	4
KEGG	hsa05010	Alzheimer disease	0.012509826	PSMA5/ATP2A2/UQCRC2/NDUFA13	4
KEGG	hsa05012	Parkinson disease	0.025391473	PSMA5/UQCRC2/NDUFA13	3

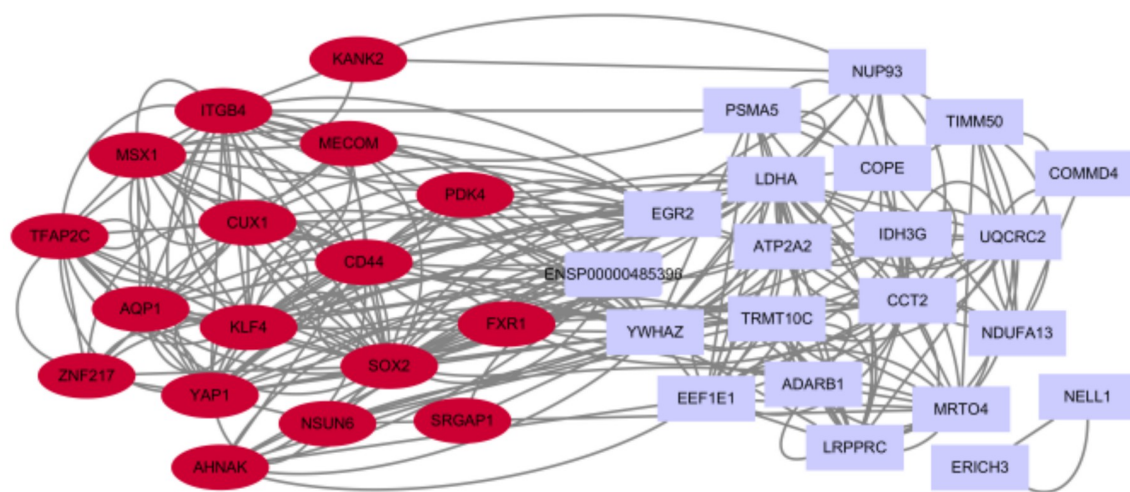
<https://doi.org/10.1371/journal.pone.0289068.t001>

Subsequently, the gene expression scores of hub genes in different regions of brain tissue were compared using the data originating from the BGEE database (Fig 7B). The brain regions are presented as follows: Hippocampal formation, Thalamus, Hypothalamus and Cerebellum. The results suggested the high and low gene expression scores of the above-described 10 hub genes in different brain regions, whereas the average and median gene expression scores reached 79.21 and 80.08, respectively. The above-mentioned hub genes were highly expressed in the brain regions studied. As revealed by the above result, the effect of m6A on AD may occur in the brain regions studied.

As indicated by the detailed data, the expression scores of SOX2, ITGB4, CD44, AQP1, and YWHAZ were higher in the respective brain region, and the expression scores of YWHAZ were higher than those of other genes, with an average expression score of 99.22. Moreover, SOX2 achieved higher expression scores in the Thalamus and Hypothalamus region, and ITGB and AQP1 achieved higher expression scores in the Hypothalamus region (both expression scores greater than 90). The data of expression scores of some genes in the database were missing. The existing data suggested that the expression scores of KLF4, EGR2, and TFAP2C in the brain tissue were all lower than 70. The expression scores of MSX1 and YAP1 ranged from 62.69 to 77.58, and no significant difference was identified between groups.

As indicated by the results of the expression of hub genes in different brain tissue regions in HPA and BGEE databases, YWHAZ and AQP1 were highly expressed in all brain tissue subregions. AQP1 was more significantly expressed in White matter, whereas YWHAZ was more highly expressed in Cerebral cortex and Hippocampal formation. SOX2, ITGB4, and CD44 were highly expressed in White matter and Hypothalamus regions.

A



B

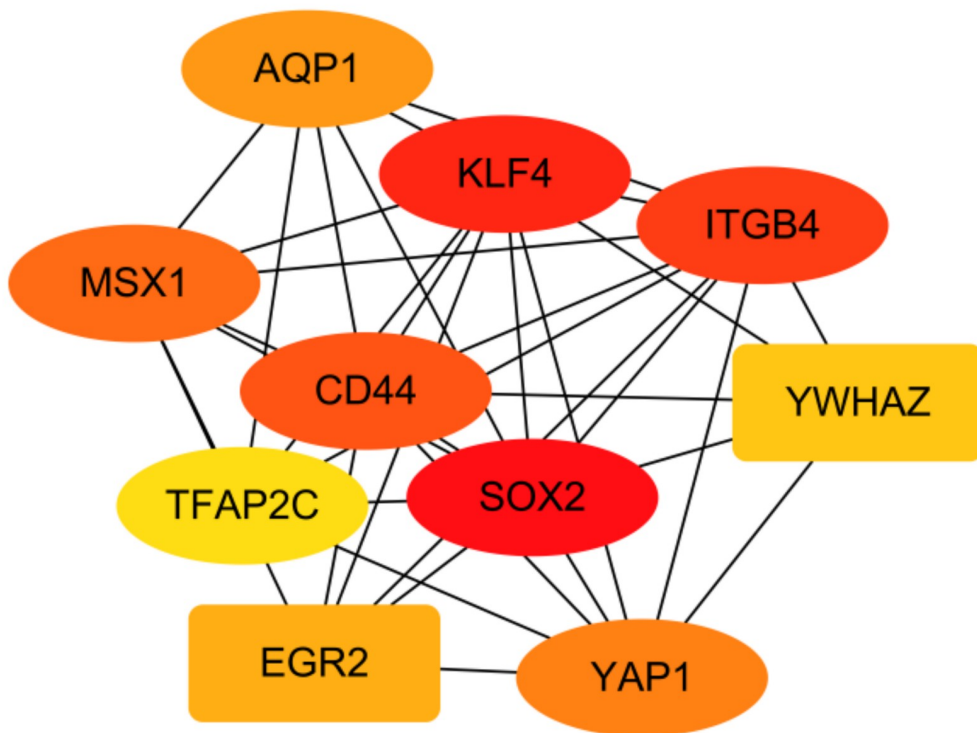


Fig 6. Construction of PPI network of the overlapping genes and screening of hub genes. (A) The PPI network of the overlapping genes of AD DGEs and m6A gene (38 nodes, 264 edges). The larger the gene degree value, the larger the point, and the darker the gene color. (B) The Cytohubba is used to construct the Top10 hub genes. The figure presents the Top10 hub genes built by the MCC method (10 nodes, 36edges).

<https://doi.org/10.1371/journal.pone.0289068.g006>

Table 2. Top 10 hub genes and their function.

Gene symbol	description	Function
SOX2	SRY-box transcription factor 2	Downstream SRRT target that mediates the promotion of neural stem cell self-renewal (By similarity); Keeps neural cells undifferentiated by counteracting the activity of proneural proteins and suppresses neuronal differentiation (By similarity).
KLF4	Krueppel-like factor 4	Transcription factor; can act both as activator and as repressor. Binds to the promoter region of its own gene and can activate its own transcription.
ITGB4	Integrin subunit beta 4	Integrin alpha-6/beta-4 is a receptor for laminin. ITGB4 binds to NRG1 (via EGF domain) and this binding is essential for NRG1-ERBB signaling
CD44	CD44 molecule	Engages, through its ectodomain, extracellular matrix components and serves as a platform for signal transduction by assembling, via its cytoplasmic domain, protein complexes containing receptor kinases and membrane proteases.
MSX1	Msh homeobox 1	Acts as a transcriptional repressor. May play a role in limb-pattern formation. Acts in craniofacial development and specifically in odontogenesis.
YAP1	Yes1 associated transcriptional regulator	Transcriptional regulator which can act both as a coactivator and a corepressor and is the critical downstream regulatory target in the Hippo signaling pathway that plays a pivotal role in organ size control.
AQP1	Aquaporin-1	Forms a water-specific channel that provides the plasma membranes of red cells and kidney proximal tubules with high permeability to water, thereby permitting water to move in the direction of an osmotic gradient.
EGR2	Early growth response 2	Sequence-specific DNA-binding transcription factor; Plays a role in hindbrain segmentation by regulating the expression of a subset of homeobox containing genes and in Schwann cell myelination by regulating the expression of genes involved in the formation and maintenance of myelin
YWHAZ	Tyrosine 3-monooxygenase/ tryptophan 5-monooxygenase activation protein zeta	Adapter protein implicated in the regulation of a large spectrum of both general and specialized signaling pathways.
TFAP2C	Transcription factor AP-2 gamma	Sequence-specific DNA-binding protein that interacts with inducible viral and cellular enhancer elements to regulate transcription of selected genes.

<https://doi.org/10.1371/journal.pone.0289068.t002>

Identification and verification of hub genes

Box plots and Scatter plot of GSE5281 and GSE48350 gene expression levels showed that hub genes expression levels were significantly different between AD and control groups (Fig 8A–8D). In the GSE5281 dataset, except KLF4, ITGB4 and CD44, there were significant differences in genes expression between the control and AD groups ($p < 0.01$). In GSE48350 dataset, except for ITGB4 and MSX1, there were significant differences in genes expression between control and AD groups ($p < 0.05$).

The diagnostic value of the 10 core genes in AD patients was assessed by using receiver operating characteristic curves, which were mutually validated in the GSE5281 and GSE48350 datasets, respectively. The AUC of all hub genes were greater than 0.500. In the GSE5281 dataset (Fig 9A), YAP1 (AUC, 0.839) had the highest value, followed by MSX1 (AUC, 0.794), TFAP2C (AUC, 0.732) and SOX2 (AUC, 0.712). In the GSE48350 dataset (Fig 9B), YWHAZ (AUC, 0.706) had the highest value, followed by SOX2 (AUC, 0.664), CD44 (AUC, 0.662), YAP1 (AUC, 0.638), and EGR2 (AUC, 0.636).

Screening for potential pharmacological targets

Prediction of potential pharmacological targets of hub genes in the cMAP database. The compounds were sorted and then screened in accordance with their scores. The first 10 drugs suggested for AD are LDN-193189, sarmentogenin, cucurbitacin-i, KI-8751, SCH-79797, AG-592, YM-155, BAX-channel-blocker, SN-38 and cercosporin (Table 3). The above-described compounds may play a therapeutic role in the course of AD.

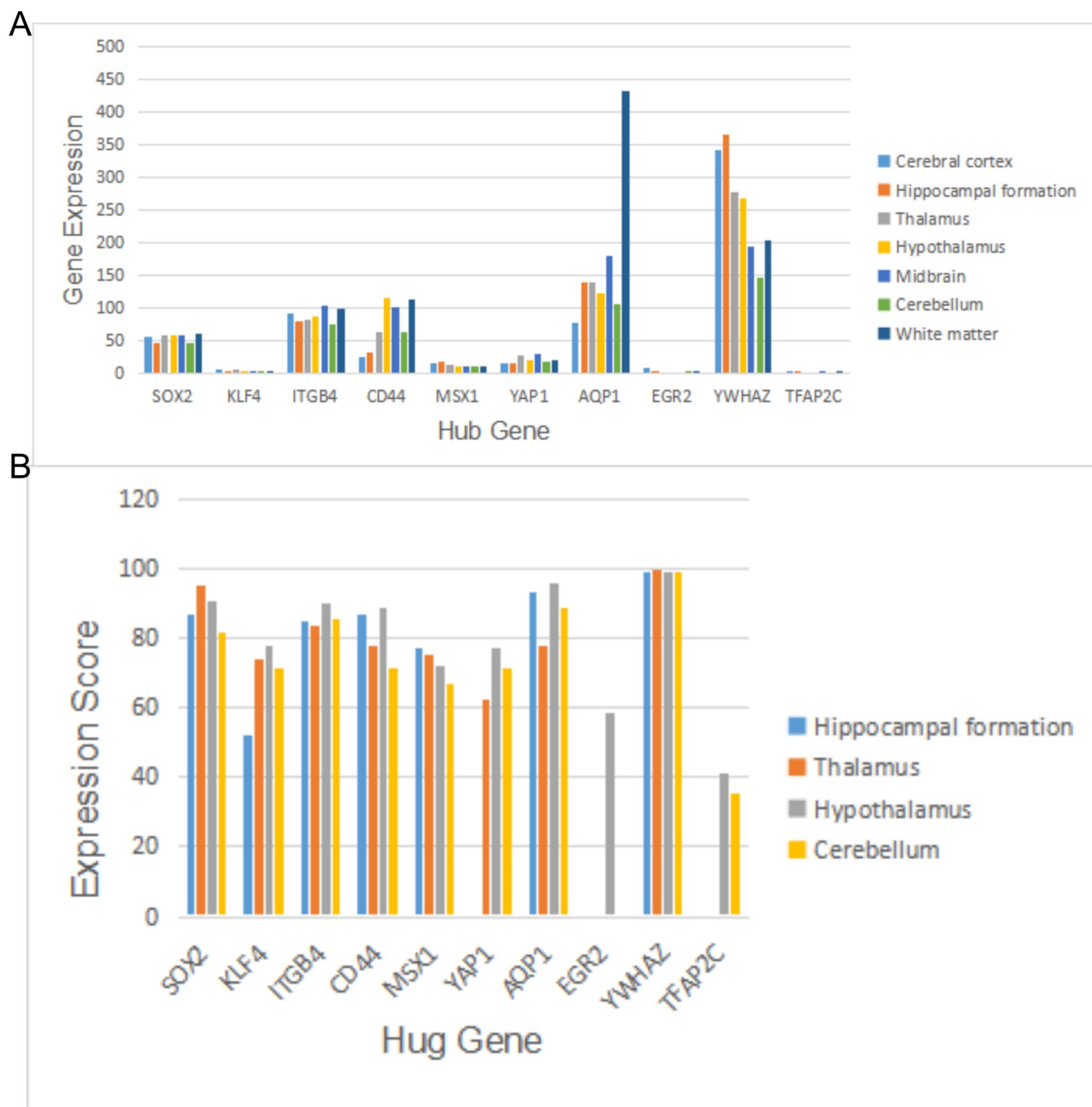


Fig 7. The expression analysis of hub genes in human brain tissues. (A) The analysis and summary of gene expression of hub genes in human brain tissues from the HPA database. (B) The gene expression scores of hub genes in different regions of the human brain tissues were compared using the Bgee database. A high score represents the gene expressed at high levels in this regions.

<https://doi.org/10.1371/journal.pone.0289068.g007>

Discussion

Alzheimer's disease refers to a neurodegenerative disorder that generally results in memory impairment and cognitive impairment [33]. Most existing research has reported that the pathological changes of AD arise from the accumulation of amyloid β plaques in the brain, mainly in the form of inflammation and tau protein aggregation in neurofibrillary tangles [34]. Several

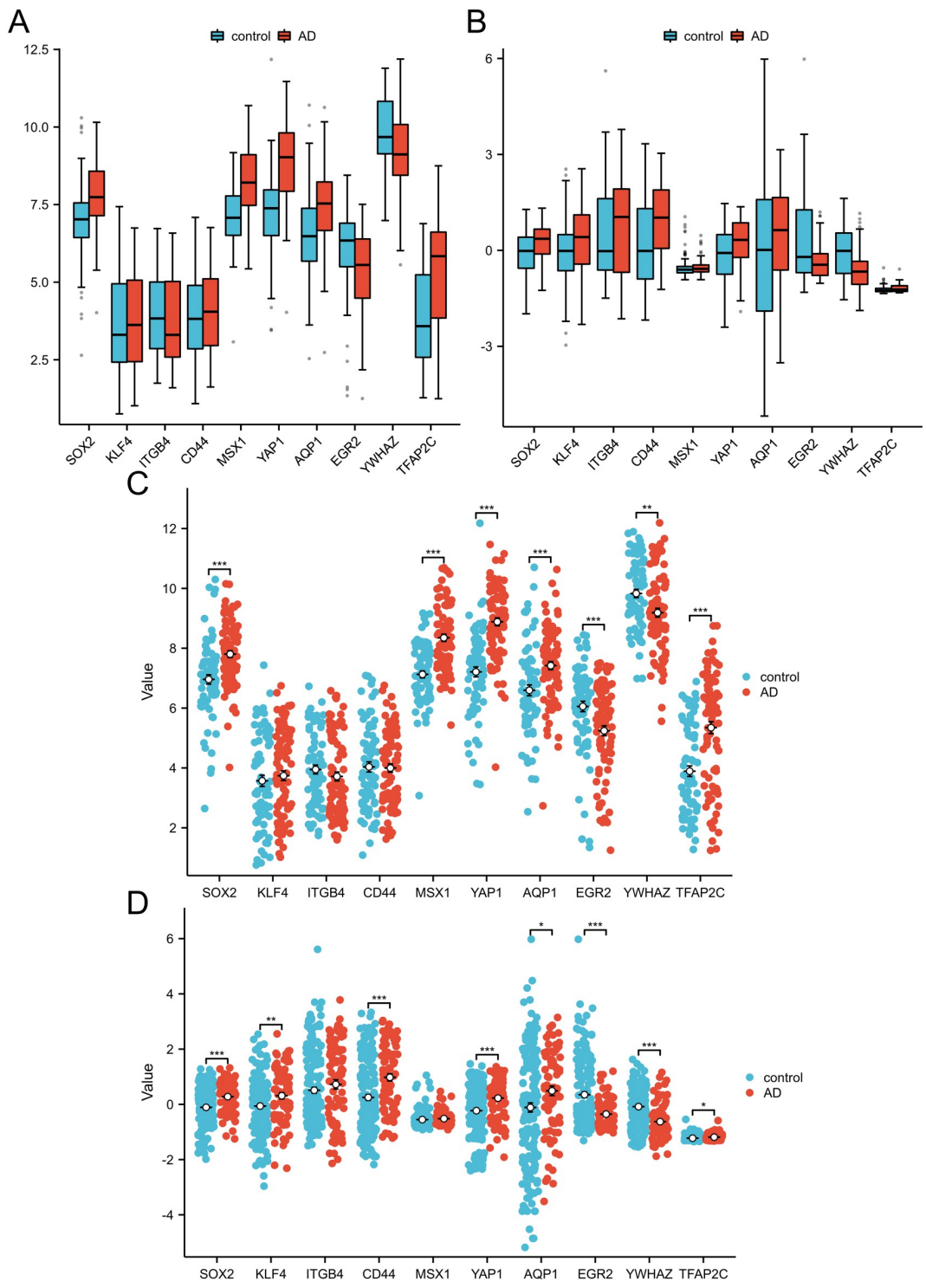


Fig 8. Comparison of the expression of 10 hub genes in AD group and normal control group. (A) Comparative expression of hub genes in the GSE5281 dataset. (B) Comparative expression of hub genes in the GSE48350 dataset. (C) Scatter plots of 10 hub genes expression in AD and control groups were compared in GSE5281 dataset. (D) Scatter plots of 10 hub genes expression in AD and control groups were compared in GSE48350 dataset. * $p < 0.05$; ** $p < 0.01$; *** $p < 0.001$.

<https://doi.org/10.1371/journal.pone.0289068.g008>

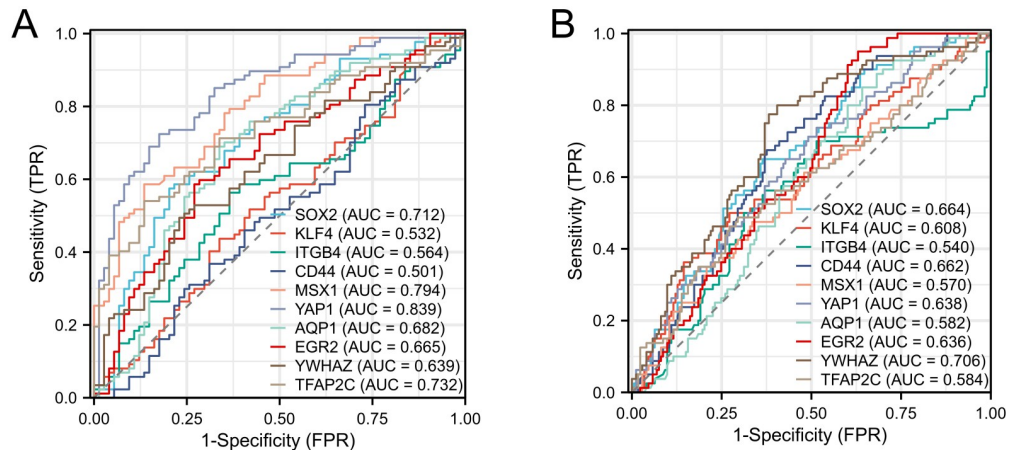


Fig 9. ROC curves of 10 hub genes. (A) Diagnostic value of hub genes in the GSE5281 dataset. (B) Diagnostic value of hub genes in the GSE48350 dataset.

<https://doi.org/10.1371/journal.pone.0289068.g009>

studies have demonstrated that m6A gene mutation and high level of gene expression show a correlation with the occurrence and development of AD [21, 22]. However, the mechanism of action remains unclear and should be studied in depth.

In this study, the brain tissue samples were first collected from AD patients from public databases, and the differentially expressed genes of m6A in AD patients' brain tissues were screened based on the analysis result of the gene expression profiling of the samples. A total of 42 DEGs were found, including 20 up-regulated genes and 22 down-regulated genes. This proves that m6A plays a role in the development of AD.

Subsequently, we performed GO and KEGG enrichment analyses on DGEs. The results of the GO analysis showed that the overlapping genes were mainly enriched in involving in retinoic acid, DNA damage response and cysteine-type endopeptidase activity of biological processes. This is consistent with previous studies. There is evidence that many steps in the retinoic acid signaling pathway, including the decline of binding proteins and metabolic enzymes, are involved in the development of AD. And there are some studies show that a

Table 3. Top 10 prediction results from cMap for AD.

Score	Name	Description
-99.71	LDN-193189	ALK inhibitor, serine/threonine protein kinase inhibitor
-98.47	sarmentogenin	ATPase inhibitor
-98.37	cucurbitacin-i	inhibitor of STAT3/JAK2 signaling, JAK inhibitor, lipocortin synthesis stimulant, STAT inhibitor
-98.15	KI-8751	PDGFR alpha and c-Kit inhibitor, vascular endothelial growth factor receptor 2 (VEGFR2) inhibitor, VEGFR inhibitor
-98.03	SCH-79797	proteinase activated receptor antagonist
-97.53	AG-592	tyrosine kinase inhibitor
-97.52	YM-155	survivin inhibitor, XIAP expression inhibitor
-97.37	BAX-channel-blocker	cytochrome C release inhibitor
-97.31	SN-38	topoisomerase inhibitor
-97.26	cercosporin	photoactivated to produce toxic reactive oxygen species, PKC inhibitor

<https://doi.org/10.1371/journal.pone.0289068.t003>

sustained decline in the mRNA and protein of retinoic acid receptors is aberrant with a decline in retinoic acid receptor β and γ transcripts at the early stages of the AD model [35, 36]. Existing research has suggested that persistent DNA damage response is a major driver of the aging phenotype, thus accelerating neuronal cell senescence and causing AD [37]. As indicated by the results of the GO analysis, the mitochondrial protein complexes were mainly enriched in involving in cellular component. Some Previous research has suggested that mitochondrial complexes are capable of inhibiting the development of AD by inducing beneficial mitochondrial stress responses [38]. A growing body of research has confirmed that RNA methylation affects neural development and aging, and dysmethylation of RNA can directly cause the neurodegenerative lesions that comprise AD [21, 39], consistent with the Molecular Function results of DGEs enrichment in this study. The result of the KEGG pathway analysis suggested that the DEGs in AD are primarily involved in Hippo signaling pathway. The Hippo signaling pathway is a mechanosensory pathway in microglia, acting through mechanization and subsequent protein kinase cascades that take on critical significance to affecting neuronal development and many other cellular processes. Hippo signaling pathway may serve as a potential therapeutic target for the prevention of microglia-induced neurodegeneration in AD [40, 41].

In addition, a protein-interaction network of m6A and AD intersecting genes was built by STRING, the PPI network was visualized using Cytoscape software, and 10 hub genes (i.e., SOX2, KLF4, ITGB4, CD44, MSX1, YAP1, AQP1, EGR2, YWHAZ, and TFAP2C) were screened using CytoHubba plug-in. SOX2 deficiency can result in neurodegeneration and injured neurons in the model rat brain. Moreover, previous research has indicated that SOX2 neural stem cells exhibit multifunction and self-renewal ability in the hippocampus of the adult model [42, 43]. KLF4 plays a vital regulatory role in the neurophysiological and neuro-pathological processes of AD [44]. KLF4 is highly expressed in the mouse model of AD. Existing research has suggested that KLF4 expression is positively correlated with extracellular deposition of amyloid- β peptide, such that AD is caused [45]. Accordingly, KLF4 may serve as a potential therapeutic target for AD. CD44, a marker for a subset of astrocyte, can be increased in the frontal cortex of AD patients, as indicated by previous research. The astrocyte also responds to neurofibrillary tangle and plaques, tau and AB in Hyperphosphorylation, and it may exert neuroprotective or deleterious effects [46]. In a weighted gene co-expression network analysis, MSX1 is highly correlated with AD phenotype in a study of key genes in Alzheimer disease, and the aged AD transgenic mice have the up-regulated expression of MSX1 [47]. Yap1 has been confirmed as one of the pivotal genes in Alzheimer's disease. It plays a certain role in upstream regulation and may prevent astrocyte aging in AD models via the CDK6 signaling pathway, such that cognitive decline can be slowed down [48, 49]. The high expression of AQP1 may impair the cognitive function of the AD model by inhibiting the Wnt signaling pathway and facilitating neuronal apoptosis. In contrast, AQP1 silencing is capable of protecting the hippocampal neurons of the AD mouse model and improving the cognitive function of AD mice [50]. As indicated by the results of existing research, EGR2 expression in the hippocampus is significantly increased in the aging process, which may play a certain role in the biological process of immune response to external stimuli [51]. Previous research has suggested that YWHAZ is directly correlated with AD. YWHAZ is significantly altered in the mouse model of AD, and it may serve as a key regulatory gene in the prefrontal cortex of AD [52]. In general, the above-mentioned 10 hub genes are potential targets for the treatment of AD.

In brief, in this study, the differentially expressed genes in AD were screened, and the overlapping genes associated with DGEs and m6A genes were identified. A total of 42 DEGs and 10 hub genes were screened. The biological changes may be correlated with retinoic acid, DNA damage response, and cysteine-type endopeptidase activity, which may occur via the Hippo signaling pathway. In this study, human brain tissue data were employed, more

consistent with the brain tissue gene expression of AD patients. Based on the research on the gene expression of 10 hub gene in different brain regions, a direction can be provided for investigating the location of m6A gene aberrant mutation in the development of AD, so as to predict potential therapeutic compounds based on hub gene and lay a theoretical basis for the in-depth study of AD therapy. Some limitations remained in this study. The differential expression, mechanism and pathway of hub gene in Alzheimer's disease, and the potential therapeutic compounds should be verified through further biological model experiments and using clinical samples.

Conclusion

In general, the potential role of m6A modification in Alzheimer's disease was investigated. The relevant hub genes (e.g., SOX2, KLF4, ITGB4, CD44, MSX1, YAP1, AQP1, EGR2, YWHAZ, and TFAP2C) and the involved pathways were identified through the bioinformatics analysis. The biological changes may be correlated with retinoic acid, DNA damage response, and cysteine-type endopeptidase activity, which may occur via the Hippo signaling pathway. Furthermore, the brain regions with high expression of hub gene were identified, and the compounds exerting potential therapeutic effects on AD were predicted. On that basis, this study can lay a theoretical basis for exploring novel therapies for AD.

Acknowledgments

The authors gratefully acknowledge the data provided by patients and researchers participating in GEO.

Author Contributions

Data curation: Pengyun Ni, Kaiting Pan.

Formal analysis: Pengyun Ni, Kaiting Pan, Bingbing Zhao.

Methodology: Pengyun Ni.

Software: Bingbing Zhao.

Writing – original draft: Pengyun Ni.

Writing – review & editing: Pengyun Ni.

References

1. Bateman RJ, Xiong C, Benzinger TL, Fagan AM, Goate A, Fox NC, et al. Dominantly Inherited Alzheimer Network. Clinical and biomarker changes in dominantly inherited Alzheimer's disease. *N Engl J Med.* 2012 Aug 30; 367(9):795–804. <https://doi.org/10.1056/NEJMoa1202753> PMID: 22784036
2. Lopez OL, Kuller LH. Epidemiology of aging and associated cognitive disorders: Prevalence and incidence of Alzheimer's disease and other dementias. *Handb Clin Neurol.* 2019; 167:139–148. <https://doi.org/10.1016/B978-0-12-804766-8.00009-1> PMID: 31753130
3. Zhang N, Ding C, Zuo Y, Peng Y, Zuo L. N6-methyladenosine and Neurological Diseases. *Mol Neurobiol.* 2022 Mar; 59(3):1925–1937. <https://doi.org/10.1007/s12035-022-02739-0> PMID: 35032318
4. Zhang C, Fu J, Zhou Y. A Review in Research Progress Concerning m6A Methylation and Immunoregulation. *Front Immunol.* 2019 Apr 26; 10:922. <https://doi.org/10.3389/fimmu.2019.00922> PMID: 31080453
5. Wang Y, Li Y, Yue M, Wang J, Kumar S, Wechsler-Reya RJ, et al. N6-methyladenosine RNA modification regulates embryonic neural stem cell self-renewal through histone modifications. *Nat Neurosci.* 2018 Feb; 21(2):195–206. <https://doi.org/10.1038/s41593-017-0057-1> PMID: 29335608

6. Wang X, Lu Z, Gomez A, Hon GC, Yue Y, Han D, et al. N6-methyladenosine-dependent regulation of messenger RNA stability. *Nature*. 2014 Jan 2; 505(7481):117–20. <https://doi.org/10.1038/nature12730> PMID: 24284625
7. Slobodin B, Han R, Calderone V, Vrielink JAFO, Loayza-Puch F, Elkon R, et al. Transcription Impacts the Efficiency of mRNA Translation via Co-transcriptional N6-adenosine Methylation. *Cell*. 2017 Apr 6; 169(2):326–337.e12. <https://doi.org/10.1016/j.cell.2017.03.031> PMID: 28388414
8. Mendel M, Delaney K, Pandey RR, Chen KM, Wenda JM, Vågbø CB, et al. Splice site m6A methylation prevents binding of U2AF35 to inhibit RNA splicing. *Cell*. 2021 Jun 10; 184(12):3125–3142.e25. <https://doi.org/10.1016/j.cell.2021.03.062> PMID: 33930289
9. Westmark CJ, Maloney B, Alisch RS, Sokol DK, Lahiri DK. FMRP Regulates the Nuclear Export of Adam9 and Psen1 mRNAs: Secondary Analysis of an N6-Methyladenosine Dataset. *Sci Rep*. 2020 Jul 1; 10(1):10781. <https://doi.org/10.1038/s41598-020-66394-y> PMID: 32612155
10. Yue H, Nie X, Yan Z, Weining S. N6-methyladenosine regulatory machinery in plants: composition, function and evolution. *Plant Biotechnol J*. 2019 Jul; 17(7):1194–1208. <https://doi.org/10.1111/pbi.13149> PMID: 31070865
11. Knuckles P, Lence T, Haussmann IU, Jacob D, Kreim N, Carl SH, et al. Zc3h13/Flacc is required for adenosine methylation by bridging the mRNA-binding factor Rbm15/Spenito to the m6A machinery component Wtap/Fli(2)d. *Genes Dev*. 2018 Mar 1; 32(5–6):415–429. <https://doi.org/10.1101/gad.309146.117> PMID: 29535189
12. Liu J, Yue Y, Han D, Wang X, Fu Y, Zhang L, et al. A METTL3-METTL14 complex mediates mammalian nuclear RNA N6-adenosine methylation. *Nat Chem Biol*. 2014 Feb; 10(2):93–5. <https://doi.org/10.1038/nchembio.1432> PMID: 24316715
13. Hu J, Manduzio S, Kang H. Epitranscriptomic RNA Methylation in Plant Development and Abiotic Stress Responses. *Front Plant Sci*. 2019 Apr 17; 10:500. <https://doi.org/10.3389/fpls.2019.00500> PMID: 31110512
14. Li A, Chen YS, Ping XL, Yang X, Xiao W, Yang Y, et al. Cytoplasmic m6A reader YTHDF3 promotes mRNA translation. *Cell Res*. 2017 Mar; 27(3):444–447. <https://doi.org/10.1038/cr.2017.10> PMID: 28106076
15. Scutenaire J, Deragon JM, Jean V, Benhamed M, Raynaud C, Favory JJ, et al. The YTH Domain Protein ECT2 Is an m6A Reader Required for Normal Trichome Branching in Arabidopsis. *Plant Cell*. 2018 May; 30(5):986–1005. <https://doi.org/10.1105/tpc.17.00854> PMID: 29618631
16. Hsu PJ, Zhu Y, Ma H, Guo Y, Shi X, Liu Y, et al. Ythdc2 is an N6-methyladenosine binding protein that regulates mammalian spermatogenesis. *Cell Res*. 2017 Sep; 27(9):1115–1127. <https://doi.org/10.1038/cr.2017.99> PMID: 28809393
17. Liu N, Zhou KI, Parisien M, Dai Q, Diatchenko L, Pan T. N6-methyladenosine alters RNA structure to regulate binding of a low-complexity protein. *Nucleic Acids Res*. 2017 Jun 2; 45(10):6051–6063. <https://doi.org/10.1093/nar/gkx141> PMID: 28334903
18. Yue Y, Liu J, He C. RNA N6-methyladenosine methylation in post-transcriptional gene expression regulation. *Genes Dev*. 2015 Jul 1; 29(13):1343–55. <https://doi.org/10.1101/gad.262766.115> PMID: 26159994
19. Lence T, Akhtar J, Bayer M, Schmid K, Spindler L, Ho CH, et al. m6A modulates neuronal functions and sex determination in Drosophila. *Nature*. 2016 Dec 8; 540(7632):242–247. <https://doi.org/10.1038/nature20568> PMID: 27919077
20. Kan L, Ott S, Joseph B, Park ES, Dai W, Kleiner RE, et al. A neural m6A/Ythdf pathway is required for learning and memory in Drosophila. *Nat Commun*. 2021 Mar 5; 12(1):1458. <https://doi.org/10.1038/s41467-021-21537-1> PMID: 33674589
21. Shafik AM, Zhang F, Guo Z, Dai Q, Pajdzik K, Li Y, et al. N6-methyladenosine dynamics in neurodevelopment and aging, and its potential role in Alzheimer's disease. *Genome Biol*. 2021 Jan 5; 22(1):17. <https://doi.org/10.1186/s13059-020-02249-z> PMID: 33402207
22. Han M, Liu Z, Xu Y, Liu X, Wang D, Li F, et al. Abnormality of m6A mRNA Methylation Is Involved in Alzheimer's Disease. *Front Neurosci*. 2020 Feb 28; 14:98. <https://doi.org/10.3389/fnins.2020.00098> PMID: 32184705
23. Barrett T, Wilhite SE, Ledoux P, Evangelista C, Kim IF, Tomashevsky M, et al. NCBI GEO: Archive for Functional Genomics Data Sets-Update. *Nucleic Acids Res* (2013) 41(Database issue):D991–5. <https://doi.org/10.1093/nar/gks1193> PMID: 23193258
24. Davis Sean, and Meltzer Paul S. GEOquery: a bridge between the Gene Expression Omnibus (GEO) and BioConductor. *Bioinformatics* 23.14 (2007): 1846–1847. <https://doi.org/10.1093/bioinformatics/btm254> PMID: 17496320
25. Ritchie ME, Phipson B, Wu D, Hu Y, Law CW, Shi W, et al. limma powers differential expression analyses for RNA-sequencing and microarray studies. *Nucleic Acids Res*. 2015 Apr 20; 43(7):e47. <https://doi.org/10.1093/nar/gkv007> PMID: 25605792

26. Gu Z, Eils R, Schlesner M. Complex heatmaps reveal patterns and correlations in multidimensional genomic data. *Bioinformatics*. 2016 Sep 15; 32(18):2847–9. <https://doi.org/10.1093/bioinformatics/btw313> PMID: 27207943
27. Grissa D, Junge A, Oprea TI, Jensen LJ. Diseases 2.0: a weekly updated database of disease-gene associations from text mining and data integration. *Database (Oxford)*. 2022 Mar 28; 2022:baac019. <https://doi.org/10.1093/database/baac019> PMID: 35348648
28. Zhou Y, Zhou B, Pache L, Chang M, Khodabakhshi AH, Tanaseichuk O, et al. Metascape provides a biologist-oriented resource for the analysis of systems-level datasets. *Nat Commun*. 2019 Apr 3; 10(1):1523. <https://doi.org/10.1038/s41467-019-09234-6> PMID: 30944313
29. Szklarczyk D, Gable AL, Nastou KC, Lyon D, Kirsch R, Pyysalo S, et al. The STRING database in 2021: customizable protein-protein networks, and functional characterization of user-uploaded gene/measurement sets. *Nucleic Acids Res*. 2021 Jan 8; 49(D1):D605–D612. <https://doi.org/10.1093/nar/gkaa1074> PMID: 33237311
30. Doncheva NT, Morris JH, Gorodkin J, Jensen LJ. Cytoscape StringApp: Network Analysis and Visualization of Proteomics Data. *J Proteome Res*. 2019 Feb 1; 18(2):623–632. <https://doi.org/10.1021/acs.jproteome.8b00702> PMID: 30450911
31. Chin CH, Chen SH, Wu HH, Ho CW, Ko MT, Lin CY. CytoHubba: identifying hub objects and sub-networks from complex interactome. *BMC Syst Biol*. 2014; 8 Suppl 4(Suppl 4):S11. <https://doi.org/10.1186/1752-0509-8-S4-S11> PMID: 25521941
32. He J, Yan H, Cai H, Li X, Guan Q, Zheng W, et al. Statistically controlled identification of differentially expressed genes in one-to-one cell line comparisons of the CMAP database for drug repositioning. *J Transl Med*. 2017 Sep 29; 15(1):198. <https://doi.org/10.1186/s12967-017-1302-9> PMID: 28962576
33. Preische O, Schultz SA, Apel A, Kuhle J, Kaeser SA, Barro C, et al. Dominantly Inherited Alzheimer Network. Serum neurofilament dynamics predicts neurodegeneration and clinical progression in pre-symptomatic Alzheimer's disease. *Nat Med*. 2019 Feb; 25(2):277–283. <https://doi.org/10.1038/s41591-018-0304-3> PMID: 30664784
34. Jack CR Jr, Bennett DA, Blennow K, Carrillo MC, Dunn B, Haeberlein SB, et al. Contributors. NIA-AA Research Framework: Toward a biological definition of Alzheimer's disease. *Alzheimers Dement*. 2018 Apr; 14(4):535–562. <https://doi.org/10.1016/j.jalz.2018.02.018> PMID: 29653606
35. Khatib T, Chisholm DR, Whiting A, Platt B, McCaffery P. Decay in Retinoic Acid Signaling in Varied Models of Alzheimer's Disease and In-Vitro Test of Novel Retinoic Acid Receptor Ligands (RAR-Ms) to Regulate Protective Genes. *J Alzheimers Dis*. 2020; 73(3):935–954. <https://doi.org/10.3233/JAD-190931> PMID: 31884477
36. Kawahara K, Suenobu M, Ohtsuka H, Kuniyasu A, Sugimoto Y, Nakagomi M, et al. Cooperative therapeutic action of retinoic acid receptor and retinoid x receptor agonists in a mouse model of Alzheimer's disease. *J Alzheimers Dis*. 2014; 42(2):587–605. <https://doi.org/10.3233/JAD-132720> PMID: 24916544
37. Wong GC, Chow KH. DNA Damage Response-Associated Cell Cycle Re-Entry and Neuronal Senescence in Brain Aging and Alzheimer's Disease. *J Alzheimers Dis*. 2022 Jul 11. <https://doi.org/10.3233/JAD-220203> PMID: 35848025
38. Trushina E, Trushin S, Hasan MF. Mitochondrial complex I as a therapeutic target for Alzheimer's disease. *Acta Pharm Sin B*. 2022 Feb; 12(2):483–495. <https://doi.org/10.1016/j.apsb.2021.11.003> PMID: 35256930
39. Zhao F, Xu Y, Gao S, Qin L, Austria Q, Siedlak SL, et al. METTL3-dependent RNA m6A dysregulation contributes to neurodegeneration in Alzheimer's disease through aberrant cell cycle events. *Mol Neurodegener*. 2021 Sep 30; 16(1):70. <https://doi.org/10.1186/s13024-021-00484-x> PMID: 34593014
40. Bruno L, Karagil S, Mahmood A, Elbediwy A, Stolinski M, Mackenzie FE. Mechanosensing and the Hippo Pathway in Microglia: A Potential Link to Alzheimer's Disease Pathogenesis? *Cells*. 2021 Nov 12; 10(11):3144. <https://doi.org/10.3390/cells10113144> PMID: 34831369
41. Okazawa H. Intracellular amyloid hypothesis for ultra-early phase pathology of Alzheimer's disease. *Neuropathology*. 2021 Apr; 41(2):93–98. <https://doi.org/10.1111/neup.12738> PMID: 33876503
42. Sarlak G, Vincent B. The Roles of the Stem Cell-Controlling Sox2 Transcription Factor: from Neuroectoderm Development to Alzheimer's Disease? *Mol Neurobiol*. 2016 Apr; 53(3):1679–1698. <https://doi.org/10.1007/s12035-015-9123-4> PMID: 25691455
43. Wu J, Hocevar M, Foss JF, Bie B, Naguib M. Activation of CB2 receptor system restores cognitive capacity and hippocampal Sox2 expression in a transgenic mouse model of Alzheimer's disease. *Eur J Pharmacol*. 2017 Sep 15; 811:12–20. <https://doi.org/10.1016/j.ejphar.2017.05.044> PMID: 28551012
44. Cheng Z, Zou X, Jin Y, Gao S, Lv J, Li B, et al. The Role of KLF4 in Alzheimer's Disease. *Front Cell Neurosci*. 2018 Sep 21; 12:325. <https://doi.org/10.3389/fncel.2018.00325> PMID: 30297986

45. Li L, Zi X, Hou D, Tu Q. Krüppel-like factor 4 regulates amyloid-β (Aβ)-induced neuroinflammation in Alzheimer's disease. *Neurosci Lett.* 2017 Mar 16; 643:131–137. <https://doi.org/10.1016/j.neulet.2017.02.034> PMID: 28337544
46. Moreno-Rodriguez M, Perez SE, Nadeem M, Malek-Ahmadi M, Mufson EJ. Frontal cortex chitinase and pentraxin neuroinflammatory alterations during the progression of Alzheimer's disease. *J Neuroinflammation.* 2020 Feb 17; 17(1):58. <https://doi.org/10.1186/s12974-020-1723-x> PMID: 32066474
47. Liang JW, Fang ZY, Huang Y, Liuyang ZY, Zhang XL, Wang JL, et al. Application of Weighted Gene Co-Expression Network Analysis to Explore the Key Genes in Alzheimer's Disease. *J Alzheimers Dis.* 2018; 65(4):1353–1364. <https://doi.org/10.3233/JAD-180400> PMID: 30124448
48. Xu M, Zhang DF, Luo R, Wu Y, Zhou H, Kong LL, et al. A systematic integrated analysis of brain expression profiles reveals YAP1 and other prioritized hub genes as important upstream regulators in Alzheimer's disease. *Alzheimers Dement.* 2018 Feb; 14(2):215–229. <https://doi.org/10.1016/j.jalz.2017.08.012> PMID: 28923553
49. Xu X, Shen X, Wang J, Feng W, Wang M, Miao X, et al. YAP prevents premature senescence of astrocytes and cognitive decline of Alzheimer's disease through regulating CDK6 signaling. *Aging Cell.* 2021 Sep; 20(9):e13465. <https://doi.org/10.1111/acel.13465> PMID: 34415667
50. Yu B, Zhang J, Li H, Sun X. Silencing of aquaporin1 activates the Wnt signaling pathway to improve cognitive function in a mouse model of Alzheimer's disease. *Gene.* 2020 Sep 10; 755:144904. <https://doi.org/10.1016/j.gene.2020.144904> PMID: 32540373
51. Su D, Li W, Chi H, Yang H, She X, Wang K, et al. Transcriptome analysis of the hippocampus in environmental noise-exposed SAMP8 mice reveals regulatory pathways associated with Alzheimer's disease neuropathology. *Environ Health Prev Med.* 2020 Jan 9; 25(1):3. <https://doi.org/10.1186/s12199-019-0840-6> PMID: 31918655
52. Yang F, Diao X, Wang F, Wang Q, Sun J, Zhou Y, et al. Identification of Key Regulatory Genes and Pathways in Prefrontal Cortex of Alzheimer's Disease. *Interdiscip Sci.* 2020 Mar; 12(1):90–98. <https://doi.org/10.1007/s12539-019-00353-8> PMID: 32006383